

Globular Cluster System erosion in elliptical galaxies

R. Capuzzo-Dolcetta¹ and A. Mastrobuono-Battisti¹

Dep. of Physics, Sapienza, University of Roma, P.le A. Moro 5, I-00185, Roma, Italy

e-mail: roberto.capuzzodolcetta@uniroma1.it e-mail: alessandra.mastrobuonobattisti@uniroma1.it *

Received ...; accepted ...

ABSTRACT

Context. In this paper we analyze data of 8 elliptical galaxies in order to study the difference between their globular cluster systems (GCSs) radial distributions and those of the galactic stellar component. In all the galaxies studied here the globular cluster system density profile is significantly flatter toward the galactic centre than that of stars.

Aims. A flatter profile of the radial distribution of globular cluster system respect to that of the galactic stellar component is a difference which has an astrophysical relevance. A quantitative comparative analysis of the profiles may give light on both galaxy and globular cluster formation and evolution. If the difference is due to erosion of the globular cluster system, the missing GCs in the galactic central region may have actually merged around the galactic centre and formed, or at least increased in mass, the galactic nucleus. An observational support to this is the clear correlation between the galaxy integrated magnitude and the number of globular clusters lost and that between the central massive black hole mass and the total mass of globular clusters lost.

Methods. We fitted the stellar and globular cluster system radial profiles in a set of galaxies observed at high resolution. We saw that the globular cluster system profile is less peaked to the galactic centre than the stellar one is. Assuming this difference as due to GCS evolution starting from a radial distribution which was initially indistinguishable from that of stars, we may evaluate the number (and mass) of GCs ‘disappeared’ by a simple normalization procedure.

Results. The number of missing globular clusters is significant, ranging from 21% to 71% of their initial population abundance in the eight galaxies examined. The corresponding mass lost to the central galactic region is 7×10^7 - $1.85 \times 10^9 M_{\odot}$. All this mass carried toward central galactic regions have likely had an important feedback on the innermost galactic region, including its violent transient activity (AGN) and local massive black hole formation and growth.

Key words. galaxies: elliptical – clusters: globular

1. Introduction

Many elliptical galaxies contain more or less populous globular cluster systems (hereafter GCSs), that are, usually, less concentrated towards the galactic centre than the bulge-halo stars. A huge amount of literature dedicated to GCS identification in external galaxies and study of their properties, since the seminal review by Harris & Racine (1979). Regarding the GCS radial profiles, starting from the mentioned review, we just remind, for the sake of example, recent papers of Bassino et al. (2006), Goudfrooij et al. (2007), Lee et al. (2008), Rhode et al. (2007), Sikkema et al. (2006), Spitler, L.R. et al. (2006), Spitler, L.R. et al. (2008), Rhode & Zepf (2003), Peng et al. (2004) up to Harris et al. (2009).

Though it cannot be yet concluded that this characteristic is common to all galaxies, we may say no case, at present, is known where the halo stars are less concentrated than the GCS. Moreover, there is a general agreement that the difference between the two radial distributions is real and not caused by a selective bias.

Consequently, different hypotheses have been advanced with the purpose of explaining this feature. Among these, two seem the most probable:

(i) the difference between the two distributions reflects different formation ages of the two systems, as suggested by Harris & Racine (1979) and Racine (1991); in their opinion globular clusters originated earlier, when the density distribution was less

peaked. However, this hypothesis cannot explain why the two distributions are very similar in the outer galactic regions;

(ii) another explanation is based on the simple assumption of coeval birth of globular clusters and halo stars, with a further evolution of the GCS radial distribution, while the collisionless halo stands almost unchanged.

The GCS evolution is caused by both dynamical friction, which brings massive clusters very close to galactic centre, and tidal interaction with a compact nucleus (see for example Capuzzo-Dolcetta 1993). The combined effect of these dynamical mechanisms acts to deplete the GCSs in the central, denser, galactic regions, leaving the outer profile almost unaltered, then remaining similar to the profile of the halo stars. The efficiency of the mentioned phenomena is higher in galactic triaxial potentials (see for example Ostriker, Binney & Saha 1989; Pesce, Capuzzo-Dolcetta & Vietri 1992), in which there is a family of orbits, the ‘box’ orbits, which do not conserve any component of the angular momentum and then well populate the central galactic regions. Pesce et al. (1992) showed that globular clusters moving in box orbits lose their orbital energy at a rate an order of magnitude larger than those moving in loop orbits of comparable size and energy. These results showed the previous evaluations of the dynamical friction efficiency, based on very simplified hypotheses on the globular cluster orbit distribution that led to an overestimate of the dynamical braking time-scales. On the contrary, it has been ascertained that massive globular clusters in triaxial potentials are strongly braked during their motion and thus reach the inner regions in a relatively short

time (Capuzzo-Dolcetta 1993). There, they could have started a process of merging, giving origin to a central massive nucleus (eventually a black hole) or fed a pre-existent massive object (Ostriker et al. 1989; Capuzzo-Dolcetta 1993). Under the hypothesis that the initial GCS and halo-bulge radial distributions were the same, an accurate analysis of the observations would allow an estimate of the number of ‘missing clusters’ and therefore of the mass removed from the GCSs.

Actually, McLaughlin (1995), Capuzzo-Dolcetta & Vignola (1997), Capuzzo-Dolcetta & Tesserì (1999) and Capuzzo-Dolcetta & Donnarumma (2001), scaling the radial surface profiles of the halo stars of a galaxy to that of its GCS, estimated the number of missing globular clusters as the integral of the difference between the two radial profiles. Capuzzo-Dolcetta & Vignola (1997) and Capuzzo-Dolcetta & Tesserì (1999) suggested that the compact nuclei in our galaxy, M31 and M87, as well as those in many other galaxies, could have reasonably sucked in a lot of decayed globular clusters in the first few Gyrs of life.

In this paper we enlarge the discussion of the comparison of GCS and star distribution in galaxies, dealing with eight galaxies for which good photometric data are available in the literature such to draw reliable radial profiles.

In Sect. 2 we resume the way, discussed deeply in previously mentioned papers, to get from the compared GCS-stars radial profiles in a galaxy the number and mass of GCs disappeared due to time evolution of the GCS; in Sect. 3 we present and discuss the observational data, as well as the analytical fit expressions to the density profiles; in Sect. 4 we present the extension to the data of this work the correlation found by Capuzzo-Dolcetta & Donnarumma (2001) between the mass lost by the GCS, the host galaxy luminosity and the mass of the galactic central massive black hole. Finally, in Sect. 5 we summarize results and draw general conclusions. An error analysis of the methods used is presented in Appendix.

2. The estimate of the number and mass of globular clusters lost

Under the hypothesis that the flattening of the GCS distribution in the central region compared to the distribution of the stars in the galactic bulge, is due to an evolution of the GCS, the number of GC lost to the centre of the galaxy is obtained by the simple difference of the (normalized) density profiles integrated over the whole radial range (see McLaughlin 1995). A general discussion of the problems in evaluating the number and mass of missing clusters in this way can be found in Capuzzo-Dolcetta & Vignola (1997), Capuzzo-Dolcetta & Tesserì (1999) and Capuzzo-Dolcetta & Donnarumma (2001) and so it is not worth repeated here.

In this paper, we assume as reliable fitting function for the GCS projected radial distribution a “modified core model”, i.e. a law

$$\Sigma_{GC}(r) = \frac{\Sigma_0}{[1 + (r/r_c)^2]^\gamma} \quad (1)$$

where Σ_0 , r_c and γ are free parameters. The choice of this function to fit the GCS profiles is motivated by the good agreement found with almost all the data used for the purposes of this paper, as confirmed by, both, the local maximum deviation of the fitting formula from the observed data and the computed χ^2 . For the galaxy stellar profile, $\Sigma_s(r)$, we rely on the fitting formulas provided by the authors of the various papers where we got the

data from, that may change case by case, checking how good are the approximations to observed data.

The “initial” distribution of GCs, $\Sigma_{GC,0}(r)$, (assumed to be equal in shape to the present stellar profile), can be practically obtained by a vertical translation of the stellar profile, $\Sigma_s(r)$, to the present GCS distribution, $\Sigma_{GC}(r)$ as given by Eq. 1. We calculate the number of missing (lost) clusters as the surface integral of the difference between $\Sigma_{GC,0}(r)$ and $\Sigma_{GC}(r)$ over the radial range $[0, r_{max}]$ of difference of these two profiles:

$$N_l = 2\pi \int_0^{r_{max}} (\Sigma_{GC,0}(r) - \Sigma_{GC}(r)) r dr. \quad (2)$$

The present number of GCs, N , is obtained integrating $\Sigma_{GC}(r)$ over the radial range, $[r_{min}, R]$, covered by the observations (for the value of R we rely on the papers where we got the GCs distribution data from). The values of N obtained with this method are usually different from those given by the authors of the papers, but for the purposes of this paper what is important is the difference between N and N_l and, so, it is crucial a homogeneous way to determine them.

The initial number of GCs in a galaxy is, indeed, estimated as $N_i = N_l + N$.

The numerical values of N_l , N_i and N are functions of the fitting parameters and of the integration limits. These dependences and their contribution to the errors on the final results are discussed in Appendix.

An estimate of the mass removed from the GCS (M_l) can be obtained through the number of GCs lost, N_l , and the estimate of the mean mass of the missing globular clusters, $\langle m_l \rangle$. A priori, the determination of $\langle m_l \rangle$ needs the knowledge of the initial mass spectrum of the CGS, which has suffered of an evolutionary erosion. However, the most relevant evolutionary phenomena (tidal shocking and dynamical friction) act on opposite sides of the initial mass function, and so we expect that the mean value of the globular cluster mass has not changed very much in time (see Capuzzo-Dolcetta & Tesserì, 1997 and Capuzzo-Dolcetta & Donnarumma 2001). Hence, we can assume the present mean value of the mass of globular clusters, $\langle m \rangle$, as a good reference value for $\langle m_l \rangle$.

For NGC 4374, NGC 4406 and NGC 4636 we calculated $\langle m \rangle$ using their GC luminosity functions (GCLFs) and assuming the same typical mass-to-light ratio of GCs in our Galaxy, i.e. $(M/L)_{V,\odot} = 1.5$ for NGC 4406 and NGC 4636 or $(M/L)_{B,\odot} = 1.9$ (25) in the case of NGC 4374. For NGC 4636 we used also the mass function that represents its present distribution of GCs (see Sect. 3.8). For the remaining galaxies (NGC 1400, NGC 1407, NGC 4472, NGC 3258 and NGC 3268) there is no better way to estimate the total mass of ‘lost’ GCs than adopting as a ‘fiducial’ reference value for their mean mass, $\langle m_l \rangle$, the value, $\langle m_{MW} \rangle = 3.3 \times 10^5 M_\odot$, of the present mean GC mass in our Galaxy.

3. Data and results

The data for the study of this paper have been collected from the literature. We will analyze a set of 8 galaxies for which the GC content and the radial profile has been reliably determined and apt to our purposes.

The galaxies are: NGC 1400, NGC 1407, NGC 4472 (M 49), NGC 3268, NGC 3258, NGC 4374, NGC 4406 and NGC 4636. These galaxies go to enlarge the set of seventeen galaxies (Milky Way, M 31, M 87, NGC 1379, NGC 1399, NGC 1404, NGC

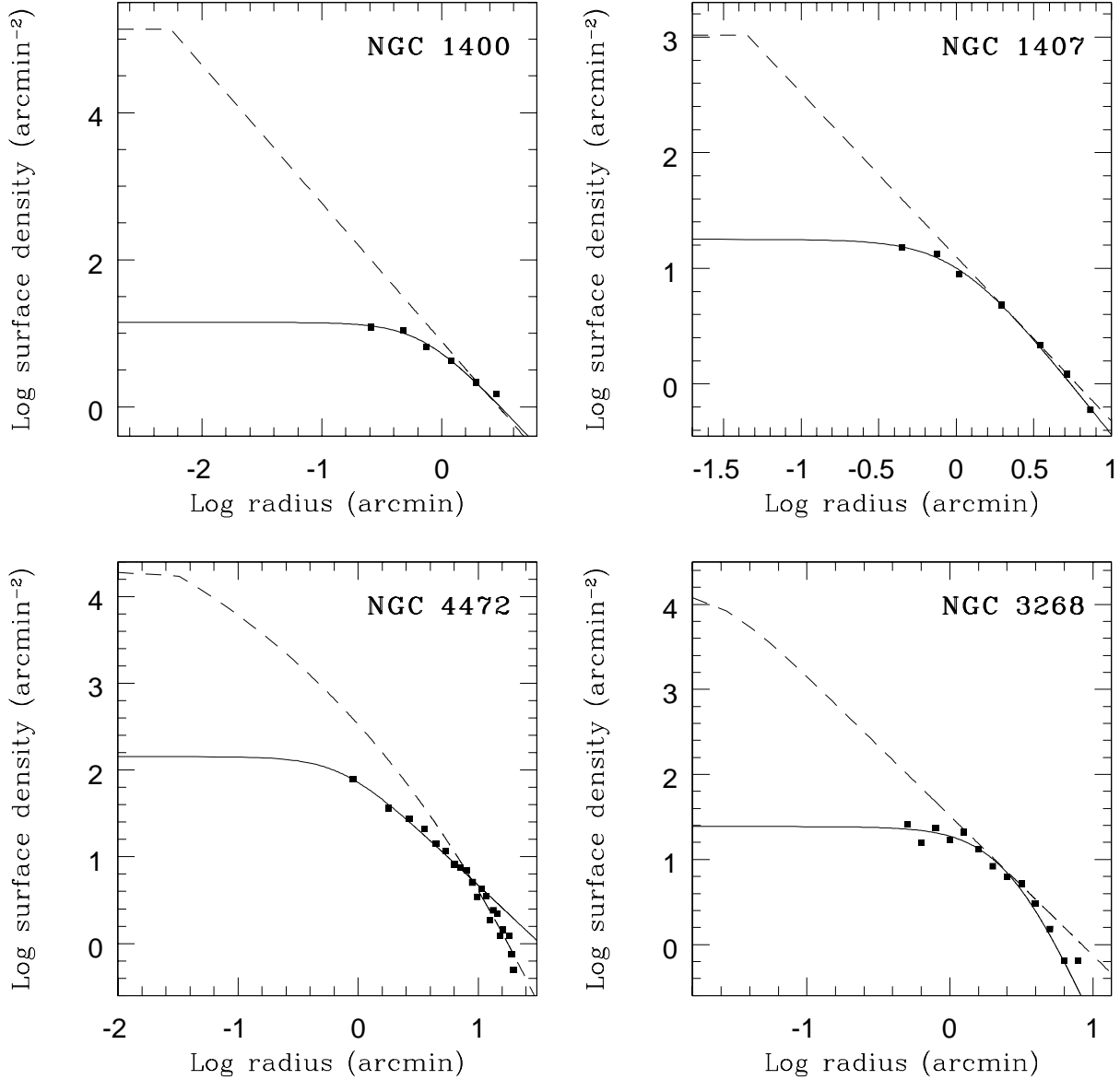


Fig. 1. Surface number density for NGC 1400, NGC 1407, NGC 4472 (M 49) and NGC 3268. Black squares represent the observed GC distribution; the solid line is its modified core model fit. The dashed curve is the surface brightness profile of the underlying galaxy (a power law and a central flat core for NGC 1400 and NGC 1407, a Sersic core model for NGC 4472 and a Nuker law for NGC 3268), vertically normalized to match the radial profile of the GCS in the outer regions.

1427, NGC 1439, NGC 1700, NGC 4365, NGC 4494, NGC 4589, NGC 5322, NGC 5813, NGC 5982, NGC 7626, IC 1459) whose GCS radial profiles have been compared to the stellar distribution in previous papers ((30), Capuzzo-Dolcetta & Vignola 1997, Capuzzo-Dolcetta & Tesserì 1999, Capuzzo-Dolcetta & Donnarumma 2001).

3.1. NGC 1400

The surface density profile of this galaxy is given by Forbes et al. (2006) (hereafter F06) who fitted it by mean of a power law $\Sigma_s(r) \propto r^{-1.88}$. This fitting law is reliable outside the galactic core, i.e. for $r > r_b = 0.0055$ arcmin (Spolaor et al. 2008). The

luminosity profile of the galaxy for $r \leq r_b$ is almost flat, and linked to the external power law. We fitted the GCS distribution by a modified core model with $\Sigma_0 = 14.1$ arcmin $^{-2}$, $r_c = 0.7$ arcmin and $\gamma = 0.88$. Integrating $\Sigma_{GC}(r)$ in the radial range where GCs are observed, i.e. from $r_{min} = 0$ arcmin to $R = 2.8$ arcmin, we obtain $N = 73$ as the present number of GC in NGC 1400. The initial GCS distribution results to be approximated by:

$$\Sigma_{GC,0}(r) = \begin{cases} 1.37 \times 10^5 \text{ arcmin}^{-2} & r \leq r_b \\ 7.76r^{-1.88} & r > r_b \end{cases} \quad (3)$$

(see Fig. 1).

Using the general method described in Sec. 2 and the estimated value $r_{max} = 2.3$ arcmin we have that the number of missing

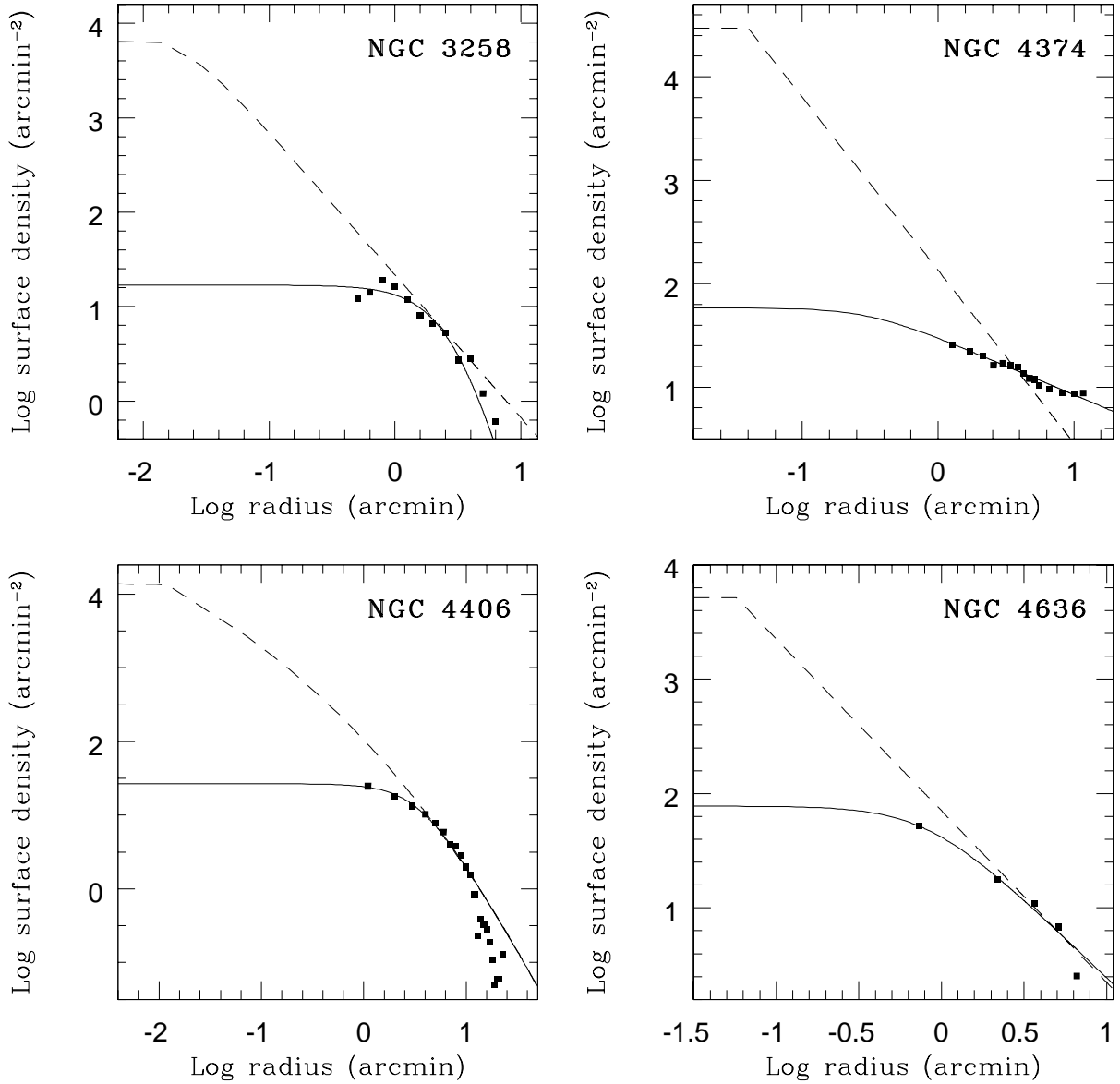


Fig. 2. Surface number density for NGC 3258, NGC 4374, NGC 4406 and NGC 4636. Black squares represent the observed GC distributions; the solid lines are their modified core model fit. The dashed curves are the surface brightness profile of the underlying galaxy (a Nuker law for NGC 3268, a power law and a central flat core for NGC 4374 and NGC 4636 and a Sersic core model for NGC 4406), vertically normalized to match the radial profile of the cluster system in the outer regions.

clusters in this galaxy is $N_l = 183$, i.e. about 71% of the initial population of globular clusters, $N_i = N_l + N = 256$. An estimate of the mass lost by the GCS is $M_l = N_l \langle m_{MW} \rangle = 6.04 \times 10^7 M_\odot$.

3.2. NGC 1407

As for NGC 1400, data for this galaxy and its GCS are taken from F06. The luminosity profile of the galaxy stars is fitted by a power law, $\Sigma_s(r) \propto r^{-1.42}$. This power law fit fails in the inner region where luminosity shows a core of radius $r_b \simeq 0.045$ arcmin (Spolaor et al. 2008). As for NGC 1400 we thus assume, for

$r \leq r_b$, a flat distribution matched to the external power law. The GCS modified core model has, in this case, $\Sigma_0 = 17.8$ arcmin $^{-2}$, $r_c = 1.02$ arcmin and $\gamma = 0.85$ as better fitting parameters. The normalizing vertical translation of the stellar profile leads to

$$\Sigma_{GC,0}(r) = \begin{cases} 1.04 \times 10^3 \text{ arcmin}^{-2} & r \leq r_b \\ 12.6r^{-1.42} & r > r_b \end{cases} \quad (4)$$

(see Fig. 1).

Integrating the difference of the GCS “initial” and present radial profiles in the galactic region where these differ, i.e. up to $r_{max} = 2.34$ arcmin (see Eq. 2), we obtain $N_l = 84$. The present number of GC obtained integrating $\Sigma_{GC}(r)$ in the radial range covered by

the observations (i.e. from 0 to $R = 7.3$ arcmin) is $N = 314$. The GCS has therefore lost 21% of its initial population, $N_i = 398$. Also in this case, we can evaluate the mass lost by the system as $M_l = N_l \langle m_{MW} \rangle = 2.77 \times 10^7 M_\odot$.

3.3. NGC 4472 (M 49)

Data for the GC distribution in this giant elliptical galaxy in Virgo are taken from Côté et al. (2003). The galaxy star luminosity distribution, according to Ferrarese et al (2006), is well reproduced by a Sersic core model (Trujillo et al. 2004), i.e. by

$$\Sigma_s(r) = \Sigma_b \left\{ \left(\frac{r_b}{r} \right)^\gamma \theta(r_b - r) + e^{b_n \left(\frac{r_b}{r_e} \right)^{\frac{1}{n}}} \theta(r - r_b) e^{-b_n \left(\frac{r}{r_e} \right)^{\frac{1}{n}}} \right\}, \quad (5)$$

where $\Sigma_s(r_b) = \Sigma_b$, $\theta(x)$ is the usual Heaviside function, r_b (break radius) divides the profile into an inner ($r \leq r_b$) power-law region and an outer ($r \geq r_b$) exponential region; r_e is the ‘effective’ radius and $b_n = 1.992n - 0.3271$, with n free fitting parameter. For M 49 the parameter values are (Côté et al. 2003): $\gamma = 0.086$, $n = 5.503$, $b_n = 10.635$, $r_e = 208$ arcsec (= 16.89 kpc), $r_b = 1.94$ arcsec (= 0.158 kpc).

In this case the core model fit to the observed GCS distribution gives $\Sigma_0 = 6 \text{ kpc}^{-2}$, $r_c = 3.57$ kpc and $\gamma = 0.652$ as optimal parameters. The usual vertical translation leads to

$$\Sigma_{GC,0}(r) = 722 \left\{ \left(\frac{0.158}{r} \right)^{0.086} \theta(0.158 - r) + 94.7 \theta(r - 0.158) e^{-10.635 \left(\frac{r}{16.89} \right)^{0.18}} \right\}. \quad (6)$$

Fig. 1 shows how the modified core model profile does not represent very well the observed GCS external profile, leading, there, to overestimate.

The surface integral (Eq. 2), performed with $r_{max} = 42.34$ kpc, gives $N_l = 5598$. Integrating $\Sigma_{GC}(r)$ up to $R = 100$ kpc we have that $N = 6334$. Hence, M 49 has lost 47% of the initial population of its GCs, $N_i = 11,932$.

As for NGC 1400 and NGC 1407, no better estimate of $\langle m_l \rangle$ is available, so we evaluate M_l as $M_l = N_l \langle m_{MW} \rangle = 1.85 \times 10^9 M_\odot$.

3.4. NGC 3268

The GC distribution of this galaxy is discussed by Dirsch, Richtler & Bassino (2003). The resulting core model fit parameters have the values: $\Sigma_0 = 24.4 \text{ arcmin}^{-2}$, $r_c = 2.6$ arcmin and $\gamma = 1.9$. The stellar luminosity profile, following Capetti & Balmaverde (2006), is well represented by a ‘Nuker’ law (introduced by Lauer et al. 1995):

$$\Sigma_s(r) = 2^{(\beta-\gamma)/\alpha} \Sigma_b \left(\frac{r_b}{r} \right)^\gamma \left[1 + \left(\frac{r}{r_b} \right)^\alpha \right]^{(\gamma-\beta)/\alpha} \quad (7)$$

where β is the slope of the external region of luminosity profile, r_b is the ‘break radius’ (corresponding to a brightness Σ_b) where the profile flattens to a smaller slope, measured by the parameter γ ; α sets the sharpness of the transition between the inner and outer profile. In the case of NGC 3268: $\alpha = 2.49$, $\beta = 1.64$, $\gamma = 0.13$ and $r_b = 0.0252$ arcmin. By the usual vertical translation of this profile, the initial GCS profile is obtained

$$\Sigma_{GC,0}(r) = 13692 \left(\frac{0.0252}{r} \right)^{0.13} \left[1 + \left(\frac{r}{0.0252} \right)^{2.49} \right]^{-0.606}. \quad (8)$$

The departure, visible in Fig. 1, of the profile given by Eq.8 from the modified core model profile in the external galactic region is mainly due to the incompleteness of the GC detection in the outermost regions. Integrating $\Sigma_{GC}(r)$ from $r_{min} = 0$ arcmin to $R = 7.94$ arcmin we have $N = 505$ as present GC number.

The number of globular clusters lost is found to be $N_l = 398$ (from 0 to $r_{max} = 2.3$ arcmin), that means about 44% of the initial abundance, $N_i = 913$.

Also in this case, to evaluate the mean mass of lost GC in NCG 3268 we have to assume $\langle m_l \rangle = \langle m_{MW} \rangle$, obtaining $M_l = N_l \langle m_{MW} \rangle = 1.31 \times 10^8 M_\odot$.

3.5. NGC 3258

As for NGC 3268 the GCS density profile data for NGC 3258 are taken from Dirsch, Richtler & Bassino (2003). The best modified core model fit is given by the values $\Sigma_0 = 16.9 \text{ arcmin}^{-2}$, $r_c = 3.1$ arcmin and $\gamma = 2.4$. The analytical fit to the luminosity profile of the galaxy is, again, obtained with the ‘Nuker’ law (Eq. (7)) with $\alpha = 2.10$, $\beta = 1.51$, $\gamma = 0$ and $r_b = 0.0192$ arcmin. By mean of the usual procedure, the initial GCS profile is obtained:

$$\Sigma_{GC,0}(r) = 8489 \left[1 + \left(\frac{r}{0.0192} \right)^{2.10} \right]^{-0.719}. \quad (9)$$

The present number of GCs is $N = 343$ (with $R = 7.94$ arcmin). Performing the surface integral of the difference of the initial and present distribution in the radial range up to $r_{max} = 2.16$ arcmin (see Eq. 2) we have $N_l = 212$, corresponding to 38% of the initial GCS population, $N_i = 555$.

For this galaxy, we obtained $M_l = N_l \langle m_{MW} \rangle = 7.00 \times 10^7 M_\odot$.

3.6. NGC 4374 (M 84)

Gomez & Richtler (2004) studied the GCS of this giant elliptical galaxy, using photometry in the B and R bands, to draw its radial surface distribution. Also in this case, the profile of the GC number density is flatter than the galaxy light (see Fig. 2). The best modified core model fit to the GC data is given by $\Sigma_0 = 58.4 \text{ arcmin}^{-2}$, $r_c = 0.31$ arcmin and $\gamma = 0.278$.

The galaxy light is characterized by a central core of radius $r_b \approx 0.0398$ arcmin (Lauer et al., 2007); for $r > r_b$, it is well fitted by the power law $\Sigma_s(r) \propto r^{-1.67}$ (Gomez & Richtler 2004). The usual normalization leads to

$$\Sigma_{GC,0}(r) = \begin{cases} 2.94 \times 10^4 \text{ arcmin}^{-2} & r \leq r_b \\ 135 r^{-1.67} & r > r_b, \end{cases} \quad (10)$$

as GCS initial radial profile. Integrating our core model up to $R = 11.8$ arcmin we get $N = 4655$ as present number of GCs. The usual integration of the difference of the initial and present GC distribution (Eq. 2 with $r_{max} = 3.84$ arcmin) leads to $N_l = 2361$. Hence NGC 4374 has lost 34% of its initial population of globular clusters, $N_i = 7016$.

In the case of NGC 4374 the value of the mean mass of a GC has been evaluated using the GCLF in the R band given by Gomez & Richtler (2004). The mean color $\langle (B - R)_0 \rangle = 1.18$ of GCs in this galaxy (Gomez & Richtler 2004) allows us to estimate the mean B absolute magnitude and the mean luminosity of GCs in the B band, $\langle (L/L_B)_\odot \rangle$ assuming $m - M = 31.61$ (Gomez & Richtler 2004). It results $\langle (L/L_B)_\odot \rangle = 1.75 \times 10^5$ (with $M_{B,\odot} = 5.47$, Cox 2000).

Adopting the mass to light ratio $(M/L)_{B,\odot} = 1.9$ obtained by Illingworth (1976) for 10 galactic globular clusters, we get $\langle m_l \rangle = 3.33 \times 10^5 M_\odot$ and $M_l = N_l \langle m_l \rangle = 7.86 \times 10^8 M_\odot$.

Galaxy	Σ_0	r_c	γ	r_{max}	R
NGC 1400	14.1	0.7	0.88	2.3	2.8
NGC 1407	17.8	1.02	0.85	2.34	7.3
NGC 4472	142	0.73	0.652	8.69	20.52
NGC 3268	24.4	2.6	1.9	2.3	7.94
NGC 3258	16.9	3.1	2.4	2.16	7.94
NGC 4374	58.4	0.31	0.278	3.84	11.8
NGC 4406	26.76	3.52	1.19	5.36	24
NGC 4636	77.66	0.823	0.691	4.75	6.6

Table 1. Col. 1: galaxy name; col. 2, 3 and 4: parameters of the modified core model fit for all the galaxies studied; col. 5: upper limit in the integral giving the number of the lost GCs (r_{max}); col. 6: upper limit of the integral performed to estimate the present number of GCs (R). Σ_0 is in arcmin^{-2} ; r_c , r_{max} and R are in arcmin.

Galaxy	Model	η	r_b	r_e	b_n	n	α	β	γ
NGC 1400	lc	7.76	5.5×10^{-3}	-	-	-	1.88	-	-
NGC 1407	lc	12.6	0.045	-	-	-	1.42	-	-
NGC 4472	cS	17139	0.0323	3.47	10.635	5.503	-	-	0.086
NGC 3268	N	13692	0.0252	-	-	-	2.49	1.64	0.13
NGC 3258	N	8489	0.0192	-	-	-	2.10	1.51	0
NGC 4374	lc	135	0.0398	-	-	-	1.67	-	-
NGC 4406	cS	13490	0.012	6.86	13.649	7.02	-	-	0.021
NGC 4636	lc	70.8	0.0573	-	-	-	1.5	-	-

Table 2. Galactic luminosity fitting parameters. Col. 1: galaxy name; col. (2) key identifying the galaxy light profile model (lc=linear with a flat core in the inner region, cS=core-Sérsic, N=Nuker); col. 3-10: parameters of the various profile models (see Sect. 2 and 3 for details). η is in arcmin^{-2} ; r_b and r_e are in arcmin.

3.7. NGC 4406 (VCC 881)

NGC 4406 is another giant elliptical in Virgo; its GCS has been studied by mean of the Mosaic Imager on the 4m Mayall telescope at the KPNO (Rhode & Zepf 2004) in the B , V and R bands. The resulting best fit core model is characterized by $\Sigma_0 = 26.76 \text{ arcmin}^{-2}$, $r_c = 3.52 \text{ arcmin}$ and $\gamma = 1.19$. The galaxy light is well fitted by a Sersic core model (Eq. 5), whose parameters have been determined by Ferrarese et al. (2006). Its vertical translation gives the initial GCS radial profile

$$\Sigma_{GC,0}(r) = 13490 \left[\left(\frac{0.012}{r} \right)^{0.021} \theta(0.012 - r) + 250\theta(r - 0.012)e^{-13.649\left(\frac{r}{0.56}\right)^{0.142}} \right]. \quad (11)$$

Integrating the present distribution of GCs, from $r_{min} = 0 \text{ arcmin}$ to $R = 24 \text{ arcmin}$, we have $N = 2850$. The surface integral given in Eq. 2, with $r_{max} = 5.36 \text{ arcmin}$, gives the number of globular clusters lost, $N_l = 1359$, i.e. about 32% of the initial GC population.

Using the GCLF of this galaxy and its distance modulus $m - M = 31.12$ (Rhode & Zepf, 2004), we evaluated the mean value of the absolute GC V magnitude, $\langle M_V \rangle = -8.42$ which corresponds to the mean luminosity $\langle L/L_\odot \rangle_V = 1.98 \times 10^5$ ($M_{V,\odot} = 4.82$ from Cox 2000).

Assuming $(M/L)_{V,\odot} = 1.5$, we obtain $\langle m_l \rangle = 2.97 \times 10^5 M_\odot$. This estimate leads to the value of the mass lost by the GCS, $M_l = N_l \langle m_l \rangle = 4.04 \times 10^8 M_\odot$.

3.8. NGC 4636

The GC content of this galaxy has been studied by Kissler Patig et al. (1994). The modified core model fit has $\Sigma_0 = 77.66 \text{ arcmin}^{-2}$, $r_c = 0.823 \text{ arcmin}$ and $\gamma = 0.691$ as optimal param-

eter values.

The galactic light profile shows an inner flat distribution (a core with radius $r_b \approx 0.0573 \text{ arcmin}$ (Lauer et al. 2007)), while for $r > r_b$ the light distribution is well fitted by the power law fit $\Sigma_s(r) \propto r^{-1.5}$ (Kissler Patig et al. 1994).

The vertical translation of the stellar profile gives the initial GCS profile:

$$\Sigma_{GC,0}(r) = \begin{cases} 5.16 \times 10^3 \text{ arcmin}^{-2} & r \leq r_b \\ 70.8r^{-1.5} & r > r_b. \end{cases} \quad (12)$$

Integrating the present surface density profile of the GCS up to $R = 6.6 \text{ arcmin}$, we obtain $N = 1411$. Performing the surface integral given in Eq. 2 (with $r_{max} = 4.75 \text{ arcmin}$), we estimate that the number of GCs disappeared is $N_l = 746$, i.e. 35% of the initial population, $N_i = 2157$. In the case of this galaxy we obtained two different estimates of the mass lost by the GCS, starting from data taken from Kissler Patig et al. (1994). The first estimate has been obtained using the GCLF (Kissler Patig et al. 1994). As for NGC 4406 we calculated the mean absolute V magnitude of GCs, $\langle M_V \rangle = -8.07$, (given $m - M = 31.2$ by Kissler Patig et al. 1994). Assuming for GCs in NGC 4636 the same M/L_V ratio of galactic GCs, $(M/L_V)_\odot = 1.5$, the deduced mean luminosity of GCs, $\langle L/L_\odot \rangle_V = 1.43 \times 10^5$, gives $\langle m_{l,1} \rangle = 2.15 \times 10^5 M_\odot$, and so $M_{l,1} = N_l \langle m_{l,1} \rangle = 1.29 \times 10^8 M_\odot$.

Another estimate is found using the mass distribution of GCs obtained in Kissler Patig et al. (1994) transforming the magnitude bins of the GCLF candidates into masses using the relation given by Mandushev et al. (1991): $\log(M/M_\odot) = -0.46M_V + 1.6$ (corresponding to a mean mass to light ratio $(M/L)_{V,\odot} \approx 2.0$). Knowing the mass distribution we can directly calculate the mean mass of GCs, $\langle m_{l,2} \rangle = 3.79 \times 10^5 M_\odot$, and thus $M_{l,2} = N_l \langle m_{l,2} \rangle = 2.97 \times 10^8 M_\odot$.

The averages of our two estimates gives $M_l = 2.22 \times 10^8 M_\odot$.

Tables 1, 2 resume the parameters of the radial profile fitting functions for the studied galaxies, while 3 resume the results in terms of estimated number and mass of GC lost.

4. The correlation between M_l , M_V and M_{bh}

The evolutionary explanation of the difference between the initial and present GC distribution implies a correlation between the (supposed) mass lost by GCS with the mass of the galactic central supermassive black hole (M_{bh}) and, likely, with the host galaxy luminosity (M_V). Tab. 4 reports the whole set of galaxies for which we have the estimate of M_V , M_{bh} and M_l .

Fig. 3 shows a plot of Tab. 4 data which clearly indicate an increasing trend of M_l as function of M_{bh} (left panel) and of M_V (right panel).

In particular, the linear fit of data in the left panel is given by $\log M_l = a \log M_{bh} + b$ with $a \pm \sigma(a) = 0.47 \pm 0.20$ and $b \pm \sigma(b) = 3.9 \pm 1.8$, giving $r = 0.45$ and $\chi^2 = 9.5$. The alternative, exponential fit gives $\log M_l = \alpha \exp(\log M_{bh}) + \beta$ where $\alpha \pm \sigma(\alpha) = (7.7 \pm 3.3) \times 10^{-5}$ and $\beta \pm \sigma(\beta) = 7.45 \pm 0.28$, $r^2 = 0.20$ and $\chi^2 = 9.6$.

We performed also fits for the correlation between M_l and M_{bh} excluding the data which have a great residual from the mean square (those of NGC 1439 and NGC 1700) obtaining the following parameters of the linear fit: $a \pm \sigma(a) = 0.61 \pm 0.15$ and $b \pm \sigma(b) = 2.9 \pm 1.3$, with $r = 0.69$ and $\chi^2 = 4.0$. The exponential fit parameters are in this case: $\alpha \pm \sigma(\alpha) = (1.17 \pm 0.22) \times 10^{-4}$ and $\beta \pm \sigma(\beta) = 7.31 \pm 0.18$, giving $r^2 = 0.60$ and $\chi^2 = 3.1$.

The least square, straight-line fit to the whole set of data shown in the right panel of Fig. 3 is given by $\log M_l = a M_V + b$ with $a \pm \sigma(a) = -0.62 \pm 0.15$ and $b \pm \sigma(b) = -5.3 \pm 3.2$, giving $r = 0.67$ and $\chi^2 = 6.6$. The exponential fit on the same data gives $\log M_l = \alpha \exp(-M_V) + \beta$ where $\alpha \pm \sigma(\alpha) = (2.20 \pm 0.49) \times 10^{-10}$ and $\beta \pm \sigma(\beta) = 7.33 \pm 0.19$, $r^2 = 0.48$ and $\chi^2 = 6.2$.

The correlation seen in the right panel of Fig. 3 between M_l and M_V reflects, both, an expected physical dependence on the total galactic mass of evolutionary processes acting on GCSs and, simply, the positive correlation between M_{bh} and M_V for the same set of galaxies. Actually, the M_{bh} - M_V correlation for the set of galaxies in Tab. 4 has a clearly positive slope, as shown also by the least square fit in Fig. 4. The least square fit is $\log M_{bh} = a M_V + b$ with $a \pm \sigma(a) = -0.56 \pm 0.15$ and $b \pm \sigma(b) = -3.41 \pm 3.22$, giving $\chi^2 = 6.54$. On the other ‘physical’ side, the energy and angular momentum dissipation caused by dynamical friction should depend on the inner galaxy phase space density ($\propto \rho/\sigma^3$, where ρ and σ are the galactic mass density and velocity dispersion, respectively). A stronger dynamical friction causes a faster GC decay toward inner galactic regions where the tidal action of a massive black hole depletes the GC population. Were brighter galaxies also denser in the phase-space, the $M_{bh} - M_V$ correlation would have a ρ/σ^3 vs. M_V counterpart. Using data available in the literature for a set of 428 galaxies (the largest part coming from a combination of data available in the catalogue by Prugniel & Simien (1996)) we find the distribution shown in the right panel of Fig. 4 which, far from being conclusive, shows indeed a trend of higher central phase space density in brighter galaxies. The least square fit is $\log(\rho/\sigma^3) = a M_V + b$ with $a \pm \sigma(a) = -0.07 \pm 0.019$ and $b \pm \sigma(b) = -1.65 \pm 0.39$, giving $\chi^2 = 194.44$.

5. Conclusions

We presented the comparative discussion of radial distribution of the globular cluster systems and of the stars in a sample of

eight elliptical galaxies observed by various authors. We find that GCS distributions flatten toward the centre, showing a broad core in the profile, contrarily to the surrounding star field. This result agrees with many previous findings, indicating, indeed, that GCs are usually less centrally concentrated than stars of the bulge-halo. A debate is still open on the interpretation of this observational issue. The ‘‘evolutionary’’ interpretation is particularly appealing; it claims that, initially, the GCS and stellar profiles were similar and, later, GCS evolved to the presently flatter distribution due to dynamical friction and tidal interactions (Capuzzo-Dolcetta 1993). In this picture, the flatter central profile is due to the erosion of the inner GCS radial profile. Many GCs are, consequently, packed in the inner galactic region, where they influence the physics of the host galaxy. Many of the galaxies studied so far have massive black holes at their centres, whose mass positively correlates with our estimates of number and mass of GC lost. This is a strong hint to the validity of the mentioned evolutionary scenario, together with the other evident correlation between number and mass of GC lost and their parent galaxy luminosity. The evolutionary hypothesis is also supported by the positive (although statistically uncertain) correlation between the (rough) estimate of the galactic central phase-space density and integrated magnitude. At the light of these encouraging findings, we think that much effort should be spent into deepening the observational tests of this astrophysical scenario.

Appendix A: The error on the estimates of number of lost GCs

Here we describe how we evaluated the errors, ϵ_l , given in Table 3. As explained in Sect. 2, the number of GCs lost in the galaxies of the sample has been evaluated as the integral of the difference between the (estimated) initial and present GCS radial distributions over the radial range $[r_{min}, r_{max}]$ where the two profiles differ. The absolute errors on N_l (ΔN_l) are given by the sum of the error on N_i (ΔN_i) and the error on N (ΔN), yielding the relative error $\epsilon_l = \frac{\Delta N_l}{N_l}$ of Table 3. We may estimate ΔN and ΔN_l as follows.

i) estimate of ΔN

For all the galaxies the number $N(r_{min}, r_{max})$ is given by

$$\begin{aligned} N(r_{min}, r_{max}) &= 2\pi \Sigma_0 \int_{r_{min}}^{r_{max}} \frac{r}{\left[1 + \left(\frac{r}{r_c}\right)^2\right]^\gamma} dr = \\ &= \frac{\Sigma_0 \pi (r^2 + r_c^2)}{(1 - \gamma) \left[1 + \left(\frac{r}{r_c}\right)^2\right]^\gamma} \Bigg|_{r_{min}}^{r_{max}} \end{aligned} \quad (\text{A.1})$$

which is a function of the parameters Σ_0 , r_c , γ , r_{min} and r_{max} whose indetermination is

$$\begin{aligned} \Delta N &= \left| \frac{\partial N}{\partial \Sigma_0} \right| \Delta \Sigma_0 + \left| \frac{\partial N}{\partial r_c} \right| \Delta r_c + \left| \frac{\partial N}{\partial \gamma} \right| \Delta \gamma + \\ &+ \left| \frac{\partial N}{\partial r_{min}} \right| \Delta r_{min} + \left| \frac{\partial N}{\partial r_{max}} \right| \Delta r_{max} \end{aligned} \quad (\text{A.2})$$

where:

$$\frac{\partial N}{\partial \Sigma_0} = 2\pi \int_{r_{min}}^{r_{max}} \frac{r}{\left[1 + \left(\frac{r}{r_c}\right)^2\right]^\gamma} dr = \frac{\pi (r^2 + r_c^2)}{(1 - \gamma) \left[1 + \left(\frac{r}{r_c}\right)^2\right]^\gamma} \Bigg|_{r_{min}}^{r_{max}}, \quad (\text{A.3})$$

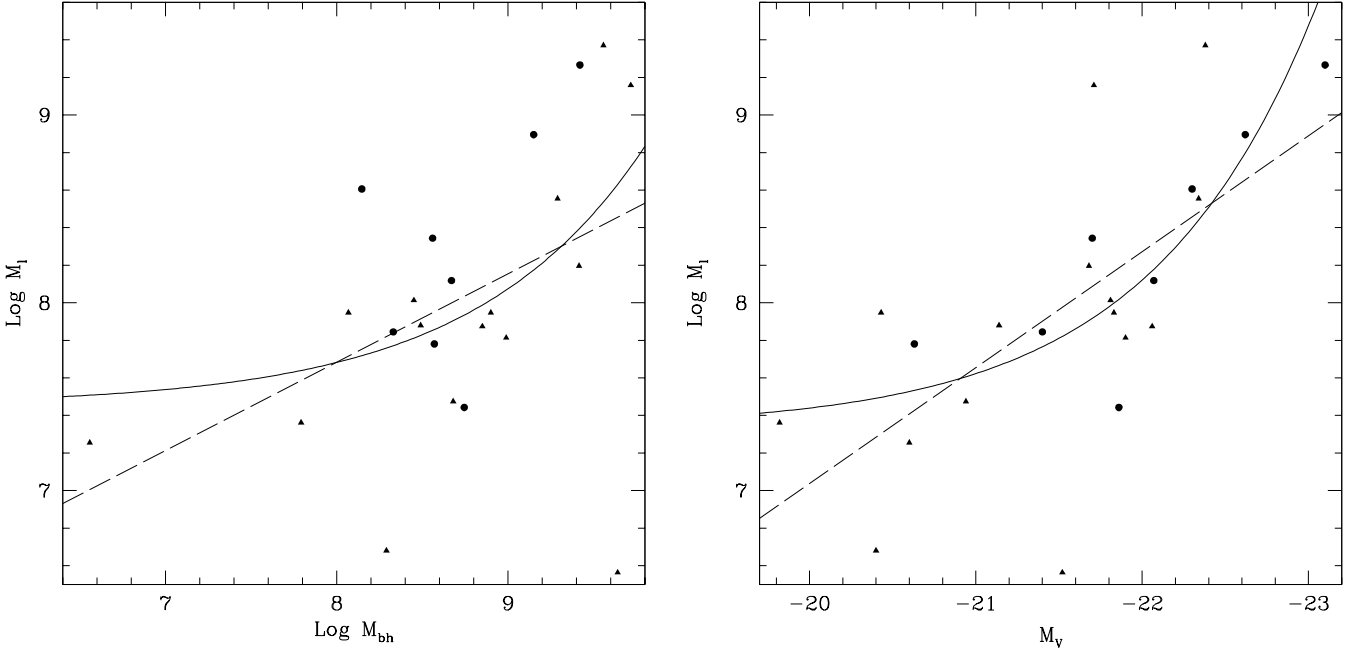


Fig. 3. The correlation between the GCS (logarithmic) mass lost and the central galactic black hole mass (left panel) and integrated V magnitude of the host galaxy (right panel) for the set of galaxies in Table 4. Masses are in solar masses. Black circles represent the eight galaxies whose GCS data are discussed in this paper, black triangles refer to the others. The straight lines and curves are the approximation fits discussed in Sect.4.

$$\begin{aligned} \frac{\partial N}{\partial r_c} &= \int_{r_{min}}^{r_{max}} \frac{4\pi\Sigma_0\gamma r^3}{r_c^3 \left[1 + \left(\frac{r}{r_c}\right)^2\right]^{(1+\gamma)}} dr = \\ &= -\frac{2\pi\Sigma_0(r_c^2 + \gamma r^2)}{r_c(\gamma - 1) \left[1 + \left(\frac{r}{r_c}\right)^2\right]^\gamma} \Bigg|_{r_{min}}^{r_{max}}, \end{aligned} \quad (\text{A.4})$$

$$\begin{aligned} \frac{\partial N}{\partial \gamma} &= -2\pi\Sigma_0 \int_{r_{min}}^{r_{max}} r \left[1 + \left(\frac{r}{r_c}\right)^2\right]^{-\gamma} \ln \left[1 + \left(\frac{r}{r_c}\right)^2\right] dr = \\ &= \frac{\pi\Sigma_0(r^2 + r_c^2) \left\{1 + (\gamma - 1) \ln \left[1 + \left(\frac{r}{r_c}\right)^2\right]\right\}}{(\gamma - 1)^2 \left[1 + \left(\frac{r}{r_c}\right)^2\right]^\gamma} \Bigg|_{r_{min}}^{r_{max}}, \end{aligned} \quad (\text{A.5})$$

$$\frac{\partial N}{\partial r_{min}} = -2\pi\Sigma_0 \frac{r_{min}}{\left[1 + \left(\frac{r_{min}}{r_c}\right)^2\right]^\gamma}, \quad (\text{A.6})$$

(we set $r_{min} = 0.1$ arcmin).

$$\frac{\partial N}{\partial r_{max}} = 2\pi\Sigma_0 \frac{r_{max}}{\left[1 + \left(\frac{r_{max}}{r_c}\right)^2\right]^\gamma}. \quad (\text{A.7})$$

The fitting parameters used to calculate ΔN are summarized in Tab. 1.

ii) estimate of ΔN_i

The fitting formulas to the initial distribution of GCS change for the various galaxies studied.

For NGC 1400, NGC 1407, NGC 4374, NGC 4636 we have (see Sect. 3.1, 3.2, 3.6, 3.8 and Tab. 2 for the meaning and the values of the parameters)

$$\begin{aligned} N_i(r_{min}, r_{max}) &= 2\pi\eta r_b^{-\alpha} \int_{r_{min}}^{r_b} r dr + 2\pi\eta \int_{r_b}^{r_{max}} r^{1-\alpha} dr = \\ &= \pi\eta r_b^{-\alpha} r^2 \Big|_{r_{min}}^{r_b} + 2\pi\eta \frac{r^{2-\alpha}}{2-\alpha} \Big|_{r_b}^{r_{max}}. \end{aligned} \quad (\text{A.8})$$

In Eq. A.8, η represents the parameter obtained by the vertical shifting of the luminosity profile.

The error ΔN_i is thus given by:

$$\Delta N_i = \left| \frac{\partial N_i}{\partial \eta} \right| \Delta \eta + \left| \frac{\partial N_i}{\partial \alpha} \right| \Delta \alpha + \left| \frac{\partial N_i}{\partial r_{min}} \right| \Delta r_{min} + \left| \frac{\partial N_i}{\partial r_{max}} \right| \Delta r_{max} \quad (\text{A.9})$$

where:

$$\begin{aligned} \frac{\partial N_i}{\partial \eta} &= 2\pi r_b^{-\alpha} \int_{r_{min}}^{r_b} r dr + 2\pi \int_{r_b}^{r_{max}} r^{1-\alpha} dr = \\ &= \pi r_b^{-\alpha} r^2 \Big|_{r_{min}}^{r_b} + 2\pi \frac{r^{2-\alpha}}{2-\alpha} \Big|_{r_b}^{r_{max}}, \end{aligned} \quad (\text{A.10})$$

$$\frac{\partial N_i}{\partial r_b} = -2\pi\eta\alpha r_b^{-1-\alpha} \int_{r_{min}}^{r_b} r dr = -\pi\eta r_b^{-1-\alpha} r^2 \Big|_{r_{min}}^{r_b}, \quad (\text{A.11})$$

$$\begin{aligned} \frac{\partial N_i}{\partial \alpha} &= -2\pi\eta r_b^{-\alpha} \int_{r_{min}}^{r_b} r \ln(r_b) dr - 2\pi\eta \int_{r_b}^{r_{max}} r^{1-\alpha} \ln(r) dr = \\ &= -2\pi r_b^{-\alpha} r^2 \ln(r_b) \Big|_{r_{min}}^{r_b} + \\ &+ \frac{2\pi\eta r^{2-\alpha} \{1 + [\alpha - 2] \ln(r)\}}{(\gamma - 2)^2} \Big|_{r_b}^{r_{max}}, \end{aligned} \quad (\text{A.12})$$

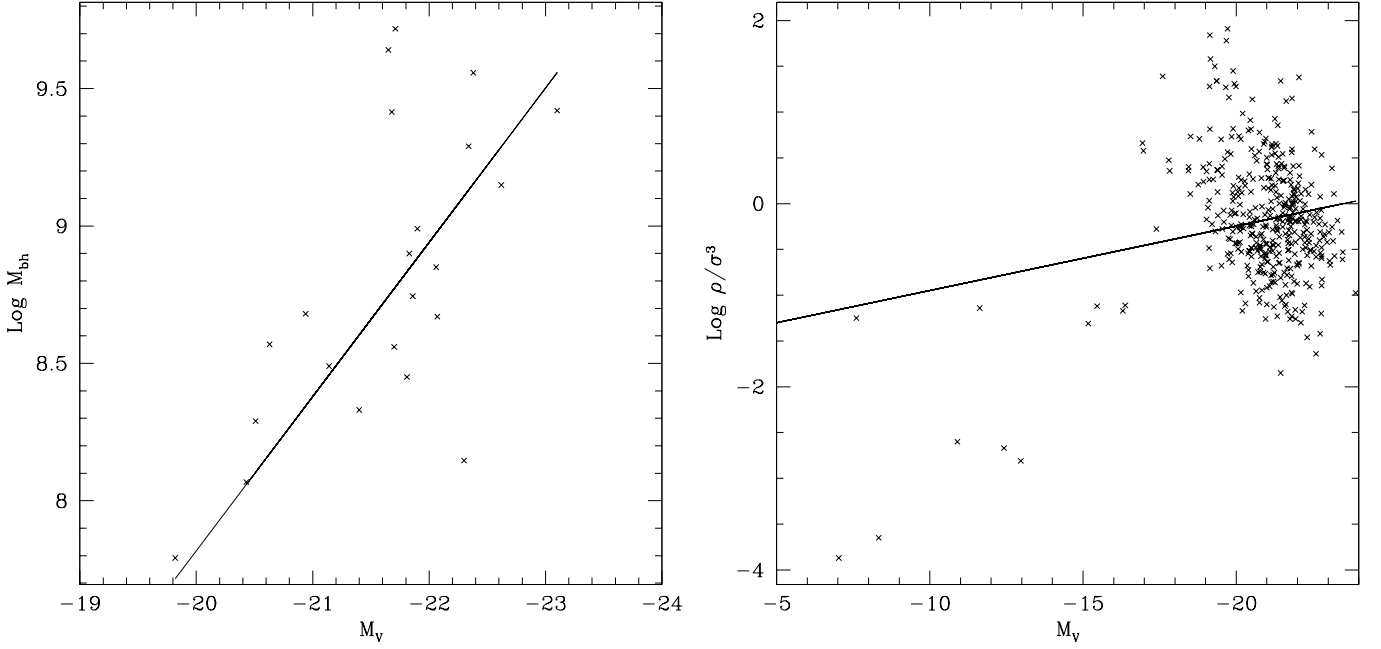


Fig. 4. Left panel: the correlation between the logarithm of the central galactic black hole mass (in solar masses) and the integrated V galactic magnitude (see Table 4). Right panel: the correlation between the value of the parameter proportional to the central galactic phase-space density (in arbitrary units) and the galactic integrated V magnitude. The straight lines are the least-square fits to the data (see Sect. 4.)

Also in this case we assumed $r_{\min} = 0.1$ arcmin. For all the galaxies analyzed, $r_{\min} > r_b$ and $r_{\max} > r_b$; so we have

$$\frac{\partial N_i}{\partial r_{\min}} = -2\pi\eta r_{\min}^{1-\alpha}, \quad (\text{A.13})$$

$$\frac{\partial N_i}{\partial r_{\max}} = 2\pi\eta r_{\max}^{1-\alpha}. \quad (\text{A.14})$$

For M 49 and NGC 4406 (Sect. 3.3 and Sect. 3.7) we have

$$\begin{aligned} N_i(r_{\min}, r_{\max}) &= \\ &= 2\pi\eta \int_{r_{\min}}^{r_{\max}} r \left\{ \left(\frac{r_b}{r} \right)^\gamma \theta(r_b - r) + e^{b_n \left[\left(\frac{r_b}{r_e} \right)^{\frac{1}{n}} - \left(\frac{r}{r_e} \right)^{\frac{1}{n}} \right]} \theta(r - r_b) \right\} dr = \\ &= \frac{2\pi\eta}{2-\gamma} r^2 \left(\frac{r_b}{r} \right)^\gamma \Big|_{r_{\min}}^{r_b} + 2\pi\eta \int_{r_b}^{r_{\max}} r e^{b_n \left[\left(\frac{r_b}{r_e} \right)^{\frac{1}{n}} - \left(\frac{r}{r_e} \right)^{\frac{1}{n}} \right]} dr \end{aligned} \quad (\text{A.15})$$

where $b_n = 1.992n - 0.3271$. The second row of the previous expression is justified by the fact that, both for M 49 and NGC 4406, $r_b > r_{\min}$. Thus the error on N_i

$$\begin{aligned} \Delta N_i &= \left| \frac{\partial N_i}{\partial \eta} \right| \Delta \eta + \left| \frac{\partial N_i}{\partial b_n} \right| \Delta b_n + \left| \frac{\partial N_i}{\partial r_b} \right| \Delta r_b + \left| \frac{\partial N_i}{\partial r_e} \right| \Delta r_e + \\ &+ \left| \frac{\partial N_i}{\partial n} \right| \Delta n + \left| \frac{\partial N_i}{\partial r_{\min}} \right| \Delta r_{\min} + \left| \frac{\partial N_i}{\partial r_{\max}} \right| \Delta r_{\max} \end{aligned} \quad (\text{A.16})$$

where $\Delta b_n = \left| \frac{\partial b_n}{\partial n} \right| \Delta n$, is evaluated by the following expressions of the individual error contribution:

$$\begin{aligned} \frac{\partial N_i}{\partial \eta} &= 2\pi \int_{r_{\min}}^{r_b} r \left(\frac{r_b}{r} \right)^\gamma dr + 2\pi \int_{r_b}^{r_{\max}} r e^{b_n \left[\left(\frac{r_b}{r_e} \right)^{\frac{1}{n}} - \left(\frac{r}{r_e} \right)^{\frac{1}{n}} \right]} dr = \\ &= \frac{2\pi}{2-\gamma} r^2 \left(\frac{r_b}{r} \right)^\gamma \Big|_{r_{\min}}^{r_b} + 2\pi \int_{r_b}^{r_{\max}} r e^{b_n \left[\left(\frac{r_b}{r_e} \right)^{\frac{1}{n}} - \left(\frac{r}{r_e} \right)^{\frac{1}{n}} \right]} dr, \end{aligned} \quad (\text{A.17})$$

$$\frac{\partial N_i}{\partial b_n} = 2\pi\eta \int_{r_b}^{r_{\max}} r e^{b_n \left[\left(\frac{r_b}{r_e} \right)^{\frac{1}{n}} - \left(\frac{r}{r_e} \right)^{\frac{1}{n}} \right]} \left[\left(\frac{r_b}{r_e} \right)^{\frac{1}{n}} - \left(\frac{r}{r_e} \right)^{\frac{1}{n}} \right] dr, \quad (\text{A.18})$$

$$\begin{aligned} \frac{\partial N_i}{\partial r_b} &= 2\pi\eta\gamma \int_{r_{\min}}^{r_b} \left(\frac{r_b}{r} \right)^{\gamma-1} dr + \\ &+ 2\pi \frac{\eta b_n}{n r_e} \int_{r_b}^{r_{\max}} r e^{b_n \left[\left(\frac{r_b}{r_e} \right)^{\frac{1}{n}} - \left(\frac{r}{r_e} \right)^{\frac{1}{n}} \right]} \left[\left(\frac{r_b}{r_e} \right)^{\frac{1}{n}-1} - \left(\frac{r}{r_e} \right)^{\frac{1}{n}-1} \right] dr = \\ &= \frac{2\pi\eta\gamma}{2-\gamma} r \left(\frac{r_b}{r} \right)^{\gamma-1} \Big|_{r_{\min}}^{r_b} + \\ &+ 2\pi \frac{\eta b_n}{n r_e} \int_{r_b}^{r_{\max}} r e^{b_n \left[\left(\frac{r_b}{r_e} \right)^{\frac{1}{n}} - \left(\frac{r}{r_e} \right)^{\frac{1}{n}} \right]} \left[\left(\frac{r_b}{r_e} \right)^{\frac{1}{n}-1} - \left(\frac{r}{r_e} \right)^{\frac{1}{n}-1} \right] dr, \end{aligned} \quad (\text{A.19})$$

$$\frac{\partial N_i}{\partial \gamma} = 2\pi\eta \int_{r_{\min}}^{r_b} r \left(\frac{r_b}{r} \right)^\gamma \ln \left(\frac{r_b}{r} \right) dr = \quad (\text{A.20})$$

$$= \frac{2\pi\eta r^2}{(\gamma-2)^2} \left(\frac{r_b}{r} \right)^\gamma \left[1 + (2-\gamma) \ln \left(\frac{r_b}{r} \right) \right] \Big|_{r_{\min}}^{r_b} \quad (\text{A.21})$$

$$\begin{aligned} \frac{\partial N_i}{\partial r_e} &= -2\pi \frac{\eta b_n}{n r_e^2} \int_{r_b}^{r_{\max}} r e^{b_n \left[\left(\frac{r_b}{r_e} \right)^{\frac{1}{n}} - \left(\frac{r}{r_e} \right)^{\frac{1}{n}} \right]} \times \\ &\times \left[r_b \left(\frac{r_b}{r_e} \right)^{\frac{1}{n}-1} - r \left(\frac{r}{r_e} \right)^{\frac{1}{n}-1} \right] dr, \end{aligned} \quad (\text{A.22})$$

$$\begin{aligned} \frac{\partial N_i}{\partial n} &= -2\pi \frac{\eta b_n}{n^2} \int_{r_b}^{r_{\max}} r e^{b_n \left[\left(\frac{r_b}{r_e} \right)^{\frac{1}{n}} - \left(\frac{r}{r_e} \right)^{\frac{1}{n}} \right]} \times \\ &\times \left[\left(\frac{r_b}{r_e} \right)^{\frac{1}{n}} \ln \left(\frac{r_b}{r_e} \right) - \left(\frac{r}{r_e} \right)^{\frac{1}{n}} \ln \left(\frac{r}{r_e} \right) \right] dr, \end{aligned} \quad (\text{A.23})$$

Remembering that, for both NGC 4472 and NGC 4406, $r_{min} > r_b$ and $r_{max} > r_b$ we can estimate the following contributions

$$\frac{\partial N_i}{\partial r_{min}} = -2\pi\eta r_{min} \exp \left\{ b_n \left[\left(\frac{r_b}{r_e} \right)^{\frac{1}{n}} - \left(\frac{r_{min}}{r_e} \right)^{\frac{1}{n}} \right] \right\}, \quad (\text{A.24})$$

$$\frac{\partial N_i}{\partial r_{max}} = 2\pi\eta r_{max} \exp \left\{ b_n \left[\left(\frac{r_b}{r_e} \right)^{\frac{1}{n}} - \left(\frac{r_{max}}{r_e} \right)^{\frac{1}{n}} \right] \right\}. \quad (\text{A.25})$$

See Tab. 2 for the values of the parameters used in the Eq. A.15-Eq.A.25.

Last for NGC 3268 and NGC 3258 (see Sect. 3.4, Sect. 3.5 and Tab. 2 for the values of the parameters) we have

$$N_i(r_{min}, r_{max}) = 2\pi\eta \int_{r_{min}}^{r_{max}} r \left(\frac{r_b}{r} \right)^\gamma \left[1 + \left(\frac{r}{r_b} \right)^\alpha \right]^{\frac{\gamma-\beta}{\alpha}} dr, \quad (\text{A.26})$$

thus the error

$$\begin{aligned} \Delta N_i = & \left| \frac{\partial N_i}{\partial \eta} \right| \Delta \eta + \left| \frac{\partial N_i}{\partial r_b} \right| \Delta r_b + \left| \frac{\partial N_i}{\partial \gamma} \right| \Delta \gamma + \left| \frac{\partial N_i}{\partial \alpha} \right| \Delta \alpha \\ & + \left| \frac{\partial N_i}{\partial \beta} \right| \Delta \beta + \left| \frac{\partial N_i}{\partial r_{min}} \right| \Delta r_{min} + \left| \frac{\partial N_i}{\partial r_{max}} \right| \Delta r_{max} \end{aligned} \quad (\text{A.27})$$

with

$$\frac{\partial N_i}{\partial \eta} = 2\pi \int_{r_{min}}^{r_{max}} r \left(\frac{r_b}{r} \right)^\gamma \left[1 + \left(\frac{r}{r_b} \right)^\alpha \right]^{\frac{\gamma-\beta}{\alpha}} dr, \quad (\text{A.28})$$

$$\begin{aligned} \frac{\partial N_i}{\partial r_b} = & 2\pi\eta \int_{r_{min}}^{r_{max}} \left[1 + \left(\frac{r}{r_b} \right)^\alpha \right]^{\frac{\gamma-\beta}{\alpha}} \left\{ \gamma \left(\frac{r_b}{r} \right)^{\gamma-1} + \right. \\ & \left. - \frac{(\gamma-\beta)}{r_b^2} r^2 \left(\frac{r_b}{r} \right)^{\gamma-\alpha+1} \left[1 + \left(\frac{r}{r_b} \right)^\alpha \right]^{-1} \right\} dr, \end{aligned} \quad (\text{A.29})$$

$$\begin{aligned} \frac{\partial N_i}{\partial \gamma} = & 2\pi\eta \int_{r_{min}}^{r_{max}} r \left(\frac{r_b}{r} \right)^\gamma \left[1 + \left(\frac{r}{r_b} \right)^\alpha \right]^{\frac{\gamma-\beta}{\alpha}} \times \\ & \times \left\{ \ln \left(\frac{r_b}{r} \right) + \frac{1}{\alpha} \ln \left[1 + \left(\frac{r}{r_b} \right)^\alpha \right] \right\} dr, \end{aligned} \quad (\text{A.30})$$

$$\begin{aligned} \frac{\partial N_i}{\partial \alpha} = & 2\pi\eta\alpha^{-1}(\gamma-\beta) \int_{r_{min}}^{r_{max}} r \left(\frac{r_b}{r} \right)^\gamma \left[1 + \left(\frac{r}{r_b} \right)^\alpha \right]^{\frac{\gamma-\beta}{\alpha}} \times \\ & \times \left\{ \left(\frac{r}{r_b} \right)^\alpha \ln \left(\frac{r}{r_b} \right) - \alpha^{-1} \ln \left[1 + \left(\frac{r}{r_b} \right)^\alpha \right] \right\} dr, \end{aligned} \quad (\text{A.31})$$

$$\begin{aligned} \frac{\partial N_i}{\partial \beta} = & 2\pi\eta\alpha^{-1} \int_{r_{min}}^{r_{max}} r \left(\frac{r_b}{r} \right)^\gamma \left[1 + \left(\frac{r}{r_b} \right)^\alpha \right]^{\frac{\gamma-\beta}{\alpha}} \times \\ & \times \ln \left[1 + \left(\frac{r}{r_b} \right)^\alpha \right] dr. \end{aligned} \quad (\text{A.32})$$

$$\frac{\partial N_i}{\partial r_{min}} = -2\pi\eta r_{min} \left(\frac{r_b}{r_{min}} \right)^\gamma \left[1 + \left(\frac{r_{min}}{r_b} \right)^\alpha \right]^{\frac{\gamma-\beta}{\alpha}}. \quad (\text{A.33})$$

with $r_{min} = 0.1$ arcmin, and

$$\frac{\partial N_i}{\partial r_{max}} = 2\pi\eta r_{max} \left(\frac{r_b}{r_{max}} \right)^\gamma \left[1 + \left(\frac{r_{max}}{r_b} \right)^\alpha \right]^{\frac{\gamma-\beta}{\alpha}}. \quad (\text{A.34})$$

All the integrals from Eq. A.15 to Eq. A.32 must be calculated numerically using the values of the parameters given in Table 2. The results listed in Table 1 are obtained assuming an error of 1% on each independent parameter used. Only in the case of NGC 3258 we assumed $\Delta\gamma = 0.001$ because Capetti & Balmaverde (2006) obtained $\gamma = 0$ from their Nuker fit, and so it is impossible to give an estimate of the error as a percentage of γ .

Acknowledgements.

References

- Balmaverde, B., Capetti, A., 2006, A&A, 447, 97, BC06
 Bassino, L. P., Faifer, F. R., Forte, J. C., Dirsch, B., Richtler, T., Geisler, D., & Schubert, Y., 2006, A&A, 451, 789
 Bertin, G., Ciotti, L., & Del Principe, M., 2002, A&A, 386, 149
 Capetti, A., Balmaverde, B., 2005, A&A, 440, 73
 Capuzzo Dolcetta, R., 1993 ApJ, 415, 616
 Capuzzo Dolcetta, R., ASP Conference Series, 285
 Capuzzo Dolcetta, R., Donnarumma, I., 2001, MNRAS, 328, 645
 Capuzzo Dolcetta, R., Tesser, A., 1997, MNRAS, 292, 808, CDT99
 Capuzzo Dolcetta, R., Tesser, A., 1999, MNRAS, 308, 961
 Capuzzo Dolcetta, R., Vicari, A., 2005, MNRAS, 356, 899
 Capuzzo Dolcetta, R., Vignola, L., 1997, A&A, 327, 130, CD97
 Carter, D., Jenkins, C. R., 1993, MNRAS, 263, 1049, CJ93
 Côté, P., McLaughlin, D. E., Cohen, J. G., Blakeslee, J. P., ApJ, 2003, 591, 850
 Cox A. N. editor, 2000, Allen's Astrophysical Quantities, 4th ed., Springer-Verlag
 Dirsh, B., Richtler T., Bassino L. P., 2003, A&A, 408, 929, D03
 Eisenhauer, F. et al., 2005, ApJ, 268, 246, E05
 Ferrarese, L., Ford H., 2005, SSRv, 116, 523, Fe05
 Ferrarese, L., Côté, P., Jord??n, A., Peng, E. W., Blakeslee, J. P., Piatek, S., Mei, S., Merritt, D., Milosavljevic, M., Tonry, J. L., West, M. J., 2006, ApJ, 164, 334
 Forbes, D. A., Franx, M., Illingworth, G. D., Carollo, C. M., 1996, ApJ, 467, 126
 Forbes, D. A., Sanchez- Blazquez, P., Phan, A. T. T., Brodie, J. P., Strader, J., Spitler, L., 2006, MNRAS, 366, 1230, F06
 Gómez, M., Richtler, T., 2004, A&A, 415, 499, GR04
 Goudfrooij, P., Schweizer, F., Gilmore, D., Whitmore, B. C., 2007, AJ, 133, 2737
 Harris, W. E., Kavelaars, J. J., Hanes, D. A., Pritchett, C. J., Baum, W. A., 2009, AJ, 137, 3314
 Harris, W. E., Racine, R., 1979, ARA&A, 17, 241
 Illingworth, G., 1976, ApJ, 204, 73
 Kissler, M., Richtler, T., Held, E. V., Grebel, E. K., Wagner, S. J., Capaccioli, M., 1994, A&A, 287, 463, KR94
 Lauer T. R., Gebhardt K., Faber S. M., Richstone D., Tremaine, S., Kormendy J., Aller M. C., Bender R., Dressler A., Filippenko A. V., Green R., Ho L. C., 2007, ApJ, 664, 226
 Lee, M. G., Park, H. S., Kim, E., Hwang, H. S., Kim, S. C., Geisler, D., 2008, ApJ, 682, 135L
 Magorrian, J., Tremaine, S., Richstone, D., Bender, R., Bower, G., Dressler, A., Faber, S. M., Gebhardt, K., Green, R., Grillmair, C., Kormendy, J., Lauer, T., 1998, AJ, 115, 2285, M98
 McLaughlin, D. E., 1995, AJ, 109, 2034
 Peng, E. W., Ford, H. C., Freeman, K. C., 2004, ApJ, 602, 705
 Prugniel P., Simien F., 1996, A&A, 309, 749
 Rhode, K. L., Zepf, S. E., 2003, AJ, 126, 2307
 Rhode, K. L., Zepf, S. E., 2004, AJ, 127, 302, RZ04
 Rhode, K. L., Katherine, L., Zepf, S. E., Kundu, A., Larner, A. N., 2007, AJ, 134, 1403
 Richstone, D., Ajhar, E. A., Bender, R., Bower, G., Dressler, A., Faber, S. M., Filippenko, A. V., Gebhardt, K., Green, R., Ho, L. C., Kormendy, J., Lauer, T. R., Magorrian, J., Tremaine, S., 1998, Nature, 395, A14, R98
 Sikkema, G., Peletier, R. F., D.Carter, Valentijn, E. A., and Balcells, M., 2006, A&A, 458, 53
 Spitler, L. R., Forbes, D. A., Strader, J., Brodie, J. P., Gallagher, J. S., 2008, MNRAS, 385, 361
 Spitler, L. R., Larsen, S. S., Strader, J., Brodie, J. P.; Forbes, D. A., Beasley, M. A., 2006, AJ, 132, 1593
 Spolaor Ma., Forbes D. A., Hau G. K. T., Proctor R. N., Brough S., 2008, MNRAS, 385, 667
 Trujillo, I., Erwin, P., Asensio Ramos, A., Graham, A. W. 2004, AJ, 127, 1917

Van der Marel, R. P., 1999, *ApJ*, 117, 744, VM99

Verdoes, G., Van der Marel, R. P., Carollo, C. M., de Zeeuw, P. T., 2000, *AJ*, 120, 1221, VV00

Zhang, Z., Xu, H., Wang, Y., An, T., Xu, Y., Wu, X. P., 2007, *ApJ*, 656, 805, Z07

Galaxy	N	N_i	N_l	δN	ϵ_l	M_i	M_l
NGC 1400	73	256	183	0.71	0.40	8.45×10^7	6.04×10^7
NGC 1407	314	398	84	0.21	0.12	1.31×10^8	2.77×10^7
NGC 4472	6334	11932	5598	0.47	0.20	3.94×10^9	1.85×10^9
NGC 3268	505	903	398	0.44	0.15	2.98×10^8	1.31×10^8
NGC 3258	343	555	212	0.38	0.16	1.83×10^8	7.00×10^7
NGC 4374	4655	7016	2361	0.34	0.050	2.34×10^9	7.86×10^8
NGC 4406	2850	4209	1359	0.32	0.23	1.25×10^9	4.04×10^8
NGC 4636	1411	2157	746	0.35	0.11	6.41×10^8	2.22×10^8

Table 3. col. (1): galaxy name; col. 2-8: the present number of GCs (N), its initial value (N_i), the number of GCs lost (N_l), the percentage of GCs lost and the estimated relative error on N_l (ϵ_l , see Appendix), the estimate of the initial mass of the whole GCS (M_i) and of the mass lost by each GCS (M_l). M_i and M_l are in solar masses.

Galaxy	M_V	M_{bh}	M_l	Sources
MW	-20.60	3.61×10^6	1.80×10^7	E05, VV00, CDV97
M 31	-19.82	6.19×10^7	2.30×10^7	M98, CDV97
M 87	-22.38	3.61×10^9	2.33×10^9	M98, CDV97
NGC 1427	-20.43	1.17×10^8	8.86×10^7	VM99, CDT99
NGC 4365	-22.06	7.08×10^8	7.48×10^7	VM99, CDT99
NGC 4494	-20.94	4.79×10^8	2.98×10^7	VM99, CDT99
NGC 4589	-21.14	3.09×10^8	7.58×10^7	VM99, CDT99
NGC 5322	-21.90	9.77×10^8	-6.51×10^7	VM99, CDT99
NGC 5813	-21.81	2.82×10^8	1.03×10^8	VM99, CDT99
NGC 5982	-21.83	7.94×10^8	8.86×10^7	VM99, CDT99
NGC 7626	-22.34	1.95×10^9	3.59×10^7	VM99, CDT99
IC 1459	-21.68	2.60×10^9	1.57×10^8	Fe05, VM99, CDT99
NGC 1439	-20.51	1.95×10^8	4.79×10^6	VM99, CDT99
NGC 1700	-21.65	4.37×10^9	3.66×10^6	VM99, CDT99
NGC 1399	-21.71	5.22×10^9	1.44×10^8	M98, CDD01
NGC 1400	-20.63	3.71×10^8	8.45×10^7	VM99, F06, CDM
NGC 1407	-21.86	5.55×10^8	1.31×10^8	Z07, F06, CDM
NGC 4472	-23.10	2.63×10^9	3.94×10^9	M98, RZ04, CDM
NGC 3268	-22.07	4.68×10^8	2.98×10^8	BC06, D03, CDM
NGC 3258	-21.40	2.14×10^8	1.83×10^8	BC06, D03, CDM
NGC 4374	-22.62	1.41×10^9	2.34×10^9	R98, GR04, CDM
NGC 4406	-22.30	1.40×10^8	1.25×10^9	CJ93, RZ04, CDM
NGC 4636	-21.70	3.63×10^8	6.41×10^8	VM99, KR94, CDM

Table 4. col. (1) galaxy name; col. (2), (3) and (4): the V absolute magnitudes, the galactic central black hole masses and the mass lost by GCSs (both in solar masses), respectively; col. (5): bibliographic reference sources for entries in col. (2), (3) and (4); CDM is the present paper, the other acronyms are defined in the References.